Cross-Section Influence on the Out-Of-Plane Behavior of Historic Masonry Walls

Simon Szabó, Bora Pulatsu, Marco Francesco Funari, and Paulo B. Lourenço

Abstract Out-of-plane (OOP) failure mechanism is a common collapse mode for unreinforced masonry walls in the lack of connections between structural members or when the wall cross-section is characterized by multiple leaves assembled without following the so-called rules of the art. Other factors influencing the OOP behavior are the transversal texture, presence of infill material, and mechanical properties of the constituent materials, i.e., unit and mortar joint mechanical properties. Furthermore, environmental conditions may negatively affect strength properties and cause aging and degradation. Currently, the main limitation of state-of-the-art tools stems from the practical difficulties of surveying the cross-section of historic masonry structures due to enormous costs and the limitations of performing destructive tests. Therefore, computational models should address the uncertainty in the material and geometrical properties to identify possible solutions for conserving historic masonry structures. This paper aims to determine the effect of cross-section geometrical morphology of unreinforced masonry walls. Throughout this study, a collection of masonry cross-sections is considered by different morphological properties, and their structural response is analyzed by performing pushover simulations with discrete element method (DEM). The effect of cross-section morphology on strength capacity and failure mechanism is critically discussed. Finally, a simple analytical equation is modified to take into account the imperfect connection of the masonry leaves.

Keywords Historic masonry structures · Out-of-plane failure · Multi-leaf masonry wall

S. Szabó (✉) · P. B. Lourenço
Department of Civil Engineering, Institute for Sustainability and Innovation in Structural Engineering, University of Minho, 4800-058 Guimarães, Portugal
e-mail: simon.szabo@civil.uminho.pt

B. Pulatsu
Department of Civil and Environmental Engineering, Carleton University, Ottawa, ON K1S 5B6, Canada

M. F. Funari
School of Sustainability, Civil and Environmental Engineering, University of Surrey, Guildford GU2 7XH, UK

© Canadian Society for Civil Engineering 2024

S. Desjardins et al. (eds.), *Proceedings of the Canadian Society for Civil Engineering Annual Conference 2023, Volume 11*, Lecture Notes in Civil Engineering 505,
https://doi.org/10.1007/978-3-031-61531-3_8

1 Introduction

Historic masonry structures (HMS) are abundant in Europe as both residential and religious monumental buildings. Given their important role for economies and societies and low structural performance under seismic actions, preventive conservation and maintenance of the HMS stand as major priorities of the overall political strategy at the European level.

Due to the (i) geographical location, (ii) raw materials availability, (iii) facilities, and (iv) workers' skills (workmanship), HMS have experienced a great variety of building techniques developed over the centuries, defining the so-called rules of art [1, 2]. In Europe, bricks or stones were usually adopted to generate various assemblages, varying in terms of bond pattern, number of leaves, etc. While the influence of the component strength on the structural behavior of HMS is relatively well studied, few research is dedicated to the influence of masonry textures. Referring to out-of-plane (OOP) failure mechanisms, a not negligible factor is the connection of masonry leaves, which controls the capacity to generate tensile strength thanks to the interlocking between blocks and their frictional properties [3, 4]. One of the main difficulties in studying such a topic is the difficulty of surveying masonry arrangements. Firstly, the walls' surfaces are sometimes covered by plaster, and, referring to architectural heritage, only a small part of the wall can be uncovered, strongly limiting the knowledge of the masonry textures. Secondly, rigorous survey can only be achieved with high costs and invasiveness [5].

Giuffré [1] and de Felice [6] investigated masonry wall cross sections with cantilever boundary conditions under lateral loads and defined relevant geometrical indices to correlate the cross-section morphology with structural behavior. In addition, Doglioni and Mirabella [7] recommended the use of the line of minimum trace to quantify the level of interlocking between the masonry leaves. Almeida et al. [8], through experimental tests, concluded how the strength capacity of multi-leaf masonry increase with the geometric regularity of the cross-section and introduced a set of geometric indices to quantify the regularity. DEM simulations by Pulatsu et al. [9] have shown the importance of through stones in the OOP behavior of multi-leaf masonry walls. de Felice [10] conducted further DEM simulations on different real masonry cross-sections and observed how monolithic behavior could be sustained with *diatons* (through-stones), only constituting 7% of the masonry cross-section.

This brief summary of related research underlines the importance of further investigations on masonry morphology and its effect on OOP fragility, especially for boundary conditions, other than cantilever. In particular, geometric indexes characterizing a masonry pattern should be defined and correlated to structural response, in order to quantitatively assess such problems. To this end, DEM simulations have been conducted on masonry wall cross-sections with different morphology and their response correlated with a simple geometric index. The paper is divided as follows. Section 2 presents the applied computational approach, and Sect. 3 discusses the setup and outcomes of the structural simulations. Finally, relevant conclusions are drawn in Sect. 4.

2 Computational Background

DEM is a discontinuum-based approach, developed by Cundall [11] and used extensively to simulate the quasi-static and dynamic behavior of masonry structures [9, 12–14]. In DEM, the masonry texture is represented by a system of discrete blocks, which can mechanically interact at contact points. The numerical procedure of DEM is based on the integration of the equations of motion to predict the movements of blocks, considering their mechanical interactions with each other. The governing differential equations are solved using the central difference method for the new translational and rotational velocities ($\dot{\boldsymbol{u}}_i^{t+}$, $\boldsymbol{\omega}_i^{t+}$) via an explicit solution scheme as written in Eq. (1).

$$\begin{aligned} \dot{\boldsymbol{u}}_i^{t+} &= \dot{\boldsymbol{u}}_i^{t-} + \frac{\Delta t}{m}\left(\sum \boldsymbol{F}_i^t - \boldsymbol{F}_d\right), \quad \boldsymbol{F}_d = \lambda \left|\boldsymbol{F}_i^t\right| \mathrm{sgn}\left(\dot{\boldsymbol{u}}^{t-}\right) \\ \boldsymbol{\omega}_i^{t+} &= \boldsymbol{\omega}_i^{t-} + \frac{\Delta t}{I}\left(\sum \boldsymbol{M}_i^t - \boldsymbol{M}_d\right), \quad \boldsymbol{M}_d = \lambda \left|\boldsymbol{M}_i^t\right| \mathrm{sgn}\left(\dot{\boldsymbol{\omega}}^{t-}\right) \end{aligned} \tag{1}$$

where $\dot{\boldsymbol{u}}$, $\boldsymbol{\omega}$, m, and I are the translation and angular velocity vectors, block mass, and moment of inertia and Δt is the time step. Furthermore, $\sum \boldsymbol{F}_i^t$ and $\sum \boldsymbol{M}_i^t$ denote the unbalanced force and moment vectors from the contacts, self-weight, and applied loads. As written in Eq. (1), the quasi-static static solutions are obtained following the Cundall's local damping formulation (detailed in [15]). Once the new velocities are computed, they are further utilized to update rigid block positions and relative contact displacements.

The action/reaction forces at the contact points are obtained through pre-defined orthogonal springs, illustrated in Fig. 1a. Throughout this research, soft contact approach is used, meaning that the overlapping between discrete blocks is controlled by the normal (k_n) and shear (k_s) contact stiffnesses, shown in Fig. 1b, c, respectively. To simulate the dry-joint action, no tensile strength in the normal direction and only frictional resistance in the tangential direction is prescribed at the contact points [16–19]. Specifically, the Coulomb-slip joint model is used in shear that is controlled by the joint friction coefficient μ.

The normal and shear contact stresses (denoted as σ and τ, respectively) are calculated from the relative contact displacements and corrected (if needed) based on the adopted stress–displacement criteria (Fig. 1). Subsequently, the contact forces

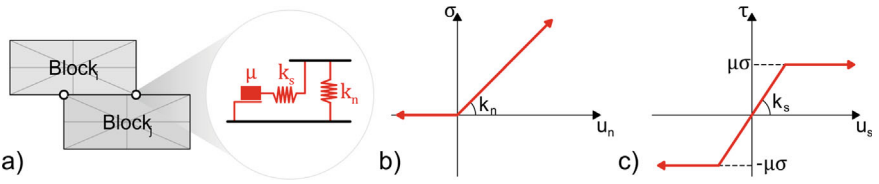

Fig. 1 **a** Illustration of point contact and defined contact constitutive laws in **b** normal and **c** shear directions

are determined by multiplying the contact stresses with the associated point-contact area. Finally, the new contact forces are used in Eq. (1). Overall, the computations are executed in a cyclic manner until a termination condition is satisfied, which generally prescribes a lower limit for the unbalanced force.

3 Analysis Design and Results

As stated above, this work aims to understand the OOP seismic behavior of two leaf masonry walls with different levels of connection between the leaves. The discussed masonry specimens are constrained at the base via pin support and at the top by a vertical roller (Fig. 2a), representing a typical boundary condition of unreinforced masonry walls of multi-story residential buildings. The specimens are subjected to gradually increasing horizontal force proportional to the mass of the blocks. Accordingly, a seismic load multiplier (λ) is obtained, which indicates the lateral load carrying capacity of the analyzed wall section.

Additionally, an analytical model consisting of two rigid blocks is considered [20], illustrated in Fig. 2b. Note that the analytical expression is derived from the virtual work principle for rigid bodies and given in Eq. (2).

$$\xi = 1 + \sqrt{2\left(\frac{W_a + W_b + N}{N}\right)} \tag{2}$$

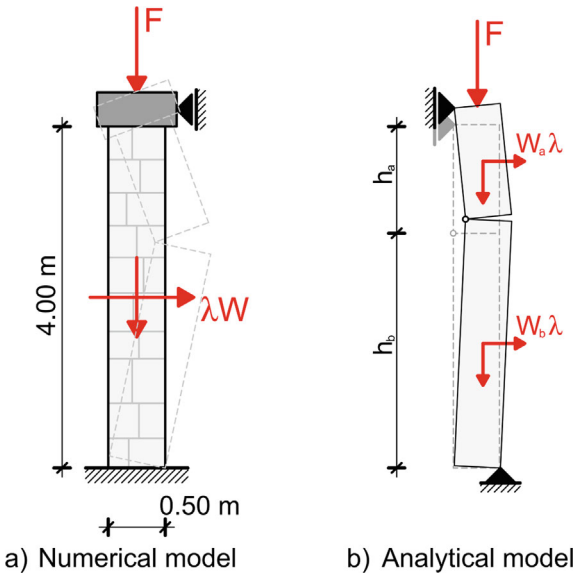

Fig. 2 Details of the test specimens in the numerical (DEM) and analytical models

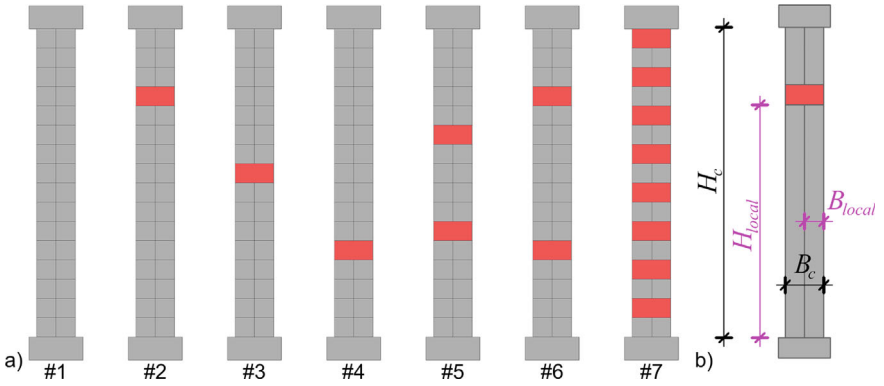

Fig. 3 Geometry of the different specimens in the numerical models

$$h_a = \left(\frac{H}{\xi}\right), \quad h_b = \left(\frac{\xi - 1}{\xi}\right)H$$
$$\lambda_{\mathrm{AN}} = \frac{B}{H}\left(\frac{2\xi + \left(\frac{N}{W_a + W_b}\right)(\xi + 1)\xi}{\xi - 1}\right) \tag{2}$$

As shown in Fig. 3a, one parent geometry with different cross-section topologies is considered by varying the position (25%, 33%, 50%, 66%, 75% of the wall height) and the number of *diatons* (1 or 2), connecting the two leaves of the wall. It should be noted how the two limiting cases of interlocking are #1, where a vertical joint is realized at the connection between leaves resulting in no load transferred among leaves, and #7, where the leaves are well connected; thus, it behaves monolithically.

To quantify the level of interlocking between the leaves of a wall, a geometric index a_χ, presented by de Felice [6], is adopted, which quantifies the lack of interlocking between leaves by measuring the slenderness of the unbounded section of the wall:

$$a_\chi = \frac{\beta_{\mathrm{local}}}{\beta_c} \tag{3}$$

where β_{local} and β_c signify the internal and global slenderness of the masonry cross-section, respectively, defined by the height-to-width ratio. β_{local} is defined from the slenderest unrestrained portion of the wall (Fig. 3b). As presented in Fig. 4a, the increase in a_χ corresponds to a reduction of the load multiplier (λ), which can be best approximated with a power formula with $R^2 = 0.9676$:

$$\lambda(a_\chi) = \lambda_7\left(0.65 \cdot a_\chi^{-0.23}\right) \tag{4}$$

where λ_7 signifies the load factor associated with perfect interlocking, as presented in Fig. 3, specimen #7.

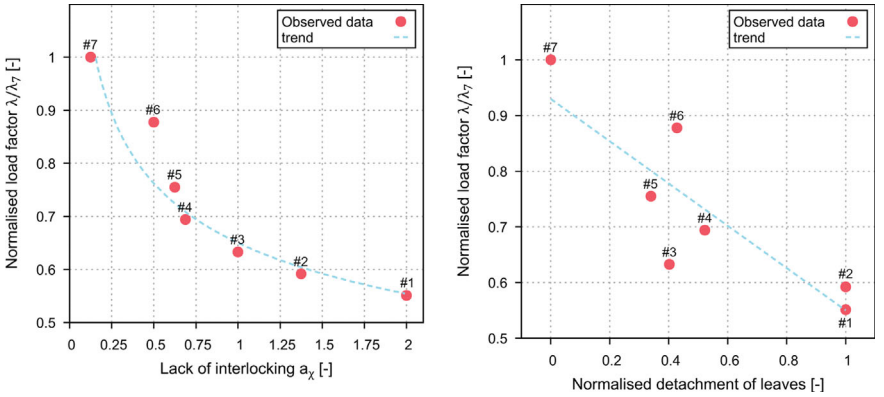

Fig. 4 Observed relation between the load factor and **a** lack of interlocking, **b** detachment of leaves parameters

It is also shown in Fig. 4b how a strong linear correlation can be observed ($R^2 = 0.726$) between the load factor and the detachment of leaves (normalized to specimen #1), defined by the area between the two leaves after the displacements. It is clear that the lower strength capacity corresponds to bigger detachment between the leaves.

Figure 5a presents the differences in displacement between the leaves of each masonry specimen. It is observed how the maximum displacement for specimens #1 and #7 occurs relatively at the same height ($\sim 2.5m$), while #1 exhibits large detachments between the leaves, compared to no detachment for #7. Specimens #2 and #4 and #6 are characterized by similar mechanism as the previous two, while due to the presence of *diatons*, the detachment of leaves is constrained to a smaller height. The height of maximum displacement reduces for #2, increases for #4 but stays the same height for #6 as compared to #1. Considering specimen #3, the wall is connected at the middle height; thus, much smaller detachments are observed in the wall. Finally, specimen #5 exhibit a mechanism, different from the other cases, with the sliding and subsequent overturning of one leaf of the top portion of the wall. In Fig. 5b, three collapse mechanisms are presented, all exhibiting predominant rocking behavior, but with differences in leaf separation and rotational hinge height.

The numerical results considering specimen #7 are observed to correspond well with the analytical solution of Eq. (2), for both the height of the rotational hinge and the load factor, as given in Table 1.

Thus, the load factor prediction of Eq. (2) can be modified with Eq. (4) to take into account limited interlocking between the leaves:

$$\lambda_{\mathrm{AN}}(a_\chi) = \lambda_{\mathrm{AN}}\left(0.65 \cdot a_\chi^{-0.23}\right) \tag{5}$$

where λ_{AN} corresponds to the analytical value of Eq. (2). On the contrary, while an evident connection can be observed between a_χ and the detachment of leaves, no clear adjustment can be made for this effect in the equation. It should also be

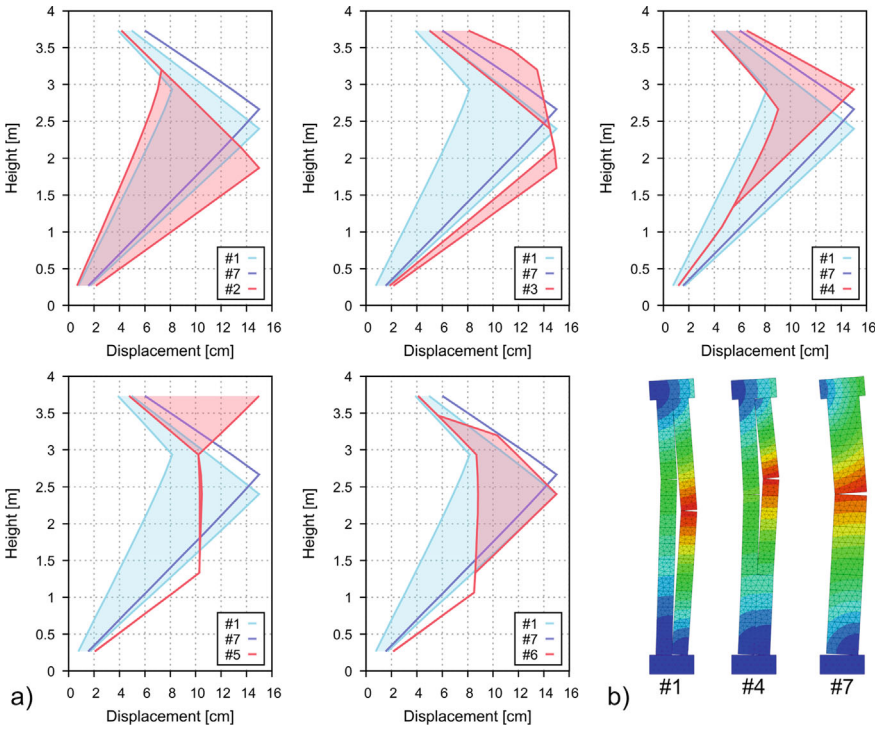

Fig. 5 Displacements of the masonry leaves

Table 1 Comparison of results from the analytical equation and numerical simulations

Response measure	Analytical equation	Simulated value	Relative error (%)
λ	2.497	2.538	−1.615
h_b	2.484 m	2.500 m	−0.64

noted that for stocky walls the provided modification may not hold true due to the predominant sliding failure mechanism.

4 Final Remarks

A discontinuum-based analysis, based on DEM, is performed on masonry wall cross-sections with different morphological properties by varying the location and height of *diatons*. The resulting horizontal load factors and detachment of leaves are compared and correlated with a geometric index, representing the lack of interlocking between the masonry leaves. A good correlation is found between the parameters, supporting

the important role of cross-section morphology on the OOP fragility of masonry walls. Finally, an analytical equation is modified to consider the lack of perfect interlocking between the masonry leaves. The present study only examines a single wall slenderness, and therefore, the results cannot be extrapolated to other cases. Further studies could examine various aspect ratios to reach a more general conclusion.

Fundings This work was partly financed by FCT/MCTES through national funds (PIDDAC) under the R&D Unit ISISE under reference UIDB/04029/2020. This study has been partly funded by the STAND4HERITAGE project that has received funding from the European Research Council (ERC) under the European Union's Horizon 2020 research and innovation programme (Grant agreement No. 833123), as an Advanced Grant. This work is also partly financed by MPP2030-FCT PhD Grants under the reference PRT/BD/154348/2022.

References

1. Giuffré A (1996) A mechanical model for statics and dynamics of historical masonry buildings. In: Protection of the architectural heritage against earthquakes. Springer, Vienna, pp 71–152
2. Szabó S, Funari MF, Lourenço PB (2023) Masonry patterns' influence on the damage assessment of URM walls: current and future trends. Dev Built Environ 13:100119. https://doi.org/10.1016/J.DIBE.2023.100119
3. Binda L, Baronio D, Penazzi M, Tiraboschi C (1999) Caratterizzazione di Murature in Pietra in Zona Sismica Data-base Sulle Sezioni Murarie e Indagini sui Materiali
4. Binda L, Fontana A, Mirabella G (1994) Mechanical behaviour and stress distribution in multiple-leaf stone walls. In: Proceedings of the 10th International Brick and Block Masonry Conference, Calgary, Alberta, Canada, pp 51–60
5. Kržan M, Gostič S, Cattari S, Bosiljkov V (2015) Acquiring reference parameters of masonry for the structural performance analysis of historical buildings. Bull Earthq Eng 13(1):203–236. https://doi.org/10.1007/s10518-014-9686-x
6. de Felice G (2005) Out-of-plane fragility of historic masonry walls. Conf Struct Anal Hist Constr
7. Doglioni F, Roberti GM (2004) Valutazione speditiva della vulnerabilità sismica di murature in pietra: un caso di studio. In: XI Congresso Nazionale "L'ingegneria Sismica in Italia", Genova, pp 25–29
8. Almeida C, Guedes JM, Coelho AJ, Arêde D (2014) Shear-Compressive experimental behaviour of one-leaf stone masonry walls in North of Portugal. Accessed: Apr. 25, 2022 [Online]. Available: https://www.researchgate.net/publication/274719517
9. Pulatsu B, Bretas EM, Lourenço PB (2016) Discrete element modeling of masonry structures: Validation and application. Earthq Struct 11(4):563–582. https://doi.org/10.12989/EAS.2016.11.4.563
10. De Felice G (2011) Out-of-plane seismic capacity of masonry depending on wall section morphology. Int J Archit Herit 5(4–5):466–482. https://doi.org/10.1080/15583058.2010.530339
11. Cundall PA (1971) A computer model for simulating progressive, large-scale movements in blocky rock systems. The International Symposium on Rock Mechanics 2:47–65
12. Lemos JV (2019) Discrete element modeling of the seismic behavior of masonry construction. Buildings 9(2):43. https://doi.org/10.3390/buildings9020043
13. Saygili O, Lemos JV (2020) Investigation of the structural dynamic behavior of the frontinus gate. Appl Sci 10(17):5821. https://doi.org/10.3390/APP10175821
14. Pulatsu B, Erdogmus E, Bretas EM, Lourenço PB (2019) In-plane static response of dry-joint masonry arch-pier structures. In: AEI 2019: Integrated Building Solutions—The National

Agenda—Proceddings Architectural Engineering National Conference 2019, pp 240–248. https://doi.org/10.1061/9780784482261.028
15. Cundall PA, Detournay C (2017) Dynamic relaxation applied to continuum and discontinuum numerical models in geomechanics. In: Rock mechanics and engineering. CRC Press, pp 57–102
16. Pulatsu B, Erdogmus E, Lourenço PB, Lemos JV, Tuncay K, Lemos JV, Simulation of the in-plane structural behavior of unreinforced masonry walls and buildings using DEM. https://doi.org/10.1016/j.istruc.2020.08.026
17. Baraldi D, Cecchi A (2017) A full 3D rigid block model for the collapse behaviour of masonry walls. Eur J Mech A/Solids 64:11–28. https://doi.org/10.1016/J.EUROMECHSOL.2017.01.012
18. Papantonopoulos C, Psycharis IN, Papastamatiou DY, Lemos JV, Mouzakis HP (2002) Numerical prediction of the earthquake response of classical columns using the distinct element method. Earthq Eng Struct Dyn 31(9):1699–1717. https://doi.org/10.1002/EQE.185
19. Malomo D, Pinho R, Penna A (2020) Numerical modelling of the out-of-plane response of full-scale brick masonry prototypes subjected to incremental dynamic shake-table tests. Eng Struct 209:110298. https://doi.org/10.1016/j.engstruct.2020.110298
20. Giuffrè A (1990) Letture sulla meccanica delle murature storiche. Kappa, Rome